

Mechanism controlling perpendicular alignment of the spindle to the axis of cell division in fission yeast

Yannick Gachet^{1,3}, Sylvie Tournier^{2,3},
Jonathan BA Millar^{2,*} and Jeremy S
Hyams^{1,4,*}

¹Department of Biology, University College London, London, UK and
²Division of Yeast Genetics, National Institute for Medical Research,
London, UK

In animal cells, the mitotic spindle is aligned perpendicular to the axis of cell division. This ensures that sister chromatids are separated to opposite sides of the cytokinetic actomyosin ring (CAR). We show that, in fission yeast, spindle rotation is dependent on the interaction of astral microtubules with the cortical actin cytoskeleton. Interaction initially occurs with a region surrounding the nucleus, which we term the astral microtubule interaction zone (AMIZ). Simultaneous contact of astral microtubules from both poles with the AMIZ directs spindle rotation and this requires both actin and two type V myosins, Myo51 and Myo52. Astral microtubules from one pole only then contact the CAR, which is located at the centre of the AMIZ. We demonstrate that the anillin homologue Mid1, which dictates correct placement of the CAR, is necessary to stabilise the mitotic spindle perpendicular to the axis of cell division. Finally, we show that the position of the mitotic spindle is monitored by a checkpoint that regulates the timing of sister chromatid separation.

The EMBO Journal (2004) 23, 1289–1300. doi:10.1038/sj.emboj.7600156; Published online 11 March 2004

Subject Categories: cell & tissue architecture; cell cycle

Keywords: actin; astral microtubules; fission yeast; latrunculin; spindle orientation

Introduction

In eukaryotic cells, the axis of cell division is aligned perpendicular to the mitotic spindle and in the centre of the cell. Spindle positioning in all cells depends on the interaction of astral microtubules with sites at the cell cortex. These microtubules are thought to impose pushing or pulling forces on the spindle poles to affect rotation or movement of the

spindle. In animal cells, specification of the division plane occurs as the mitotic spindle is formed. From micromanipulation and chemical inhibitor experiments in metazoa, several models have been put forward to explain the formation and positioning of the cleavage furrow. Although it is generally agreed that microtubules are essential for cleavage furrow formation, some studies suggest that astral microtubules are uniquely important, whereas others suggest that the central spindle alone dictates furrow position (reviewed in Rappaport, 1996; Oegema *et al*, 2000; Glotzer, 2001). More recent models suggest that centrosome separation and central spindle assembly act in redundant pathways to trigger cleavage furrow formation (Dechant and Glotzer, 2003). However, the initial cortical landmarks for furrow formation are not known.

Advances in our understanding of the mechanisms directing spindle positioning in budding yeast have come from examination of spindle behaviour in cells with different genetic backgrounds (Segal and Bloom, 2001; Kusch *et al*, 2002). These studies demonstrate that the determinants of spindle orientation are localised to the bud neck and bud tip and that these overlap with the determinants of interphase cell polarity. However, unlike in animal cells, the mitotic spindle in budding yeast is formed during S phase and the division plane is specified before cells enter mitosis. For these reasons, we have studied spindle positioning in the fission yeast *Schizosaccharomyces pombe*, in which the mitotic spindle is formed and positioned only in the M phase. In fission yeast, the nucleus is positioned in the middle of the cell in interphase and undergoes a symmetric division that gives rise to two identical daughter cells after mitosis (Hagan and Yanagida, 1997). The location of the cell division septum is dictated by the anillin homologue Mid1, which resides in the nucleus in interphase and relocates to the medial cell cortex in early mitosis (Chang *et al*, 1996; Sohrmann *et al*, 1996; Bahler *et al*, 1998; Paoletti and Chang, 2000). The fission yeast mitotic spindle is composed of 12–16 microtubules, overlapping in a central zone, that emanate from two spindle pole bodies (SPBs) embedded in opposite sides of a persistent nuclear envelope. An additional 10–12 microtubules originate from each SPB and terminate at the three kinetochores (Robinow and Marak, 1966; Tanaka and Kanbe, 1986; Ding *et al*, 1993, 1997). Visualisation of live *S. pombe* cells expressing GFP-tubulin has revealed that mitosis consists of three phases (Nabeshima *et al*, 1998; Tatebe *et al*, 2001). Phase 1 is prophase, during which a short, ~2.0 µm, spindle is formed. In phase 2, the spindle maintains this length (Yamamoto *et al*, 1999) and centromeres make frequent, rapid movements between the poles. At the end of phase 2, sister chromatids separate (anaphase A) and move back to the SPBs. Phase 3 consists entirely of anaphase B, during which the spindle elongates along the longitudinal axis of the cell (~14 µm), although it is not known how this orientation

*Corresponding author. Jonathan BA Millar, Division of Yeast Genetics, National Institute for Medical Research, The Ridgeway, Mill Hill, London NW7 1AA, UK. Tel.: +44 208 816 2367; Fax: +44 208 816 2523; E-mail: jmillar@nimr.mrc.ac.uk; or Jeremy S Hyams, Department of Biology, University College London, Gower Street, London WC1E 6BT, UK. E-mail: hyams@cict.fr

³These authors contributed equally to this work

⁴Present address: LBCMCP-CNRS UMR5088, Institut d'Exploration Fonctionnelle des Génomes (IFR109), Université Paul Sabatier, 118 route de Narbonne, 31062 Toulouse, France

Received: 29 July 2003; accepted: 17 November 2003; published online: 11 March 2004

is achieved. The cytoplasmic face of the two SPBs is associated with astral microtubules, which can exist in two configurations termed convergent and parallel (Hagan and Hyams, 1996). In either case, one end of each astral microtubule bundle is initially oriented towards the cortex at the cell mid-zone. As the spindle elongates, astral microtubules remain attached to the cortex, maintaining a fixed angle to the spindle axis. In fixed preparations, anaphase B spindles often appear bowed and it has been suggested that the astral microtubules apply force to the SPBs (Hagan and Hyams, 1996). Astral microtubule behaviour has, until now, not been studied in living fission yeast cells.

We recently described a new mitotic checkpoint in fission yeast that delays entry into anaphase when the actin cytoskeleton is disturbed (Gachet *et al*, 2001). Cells treated with the actin inhibitor latrunculin B entered mitosis normally and formed a short, misoriented spindle with absent or unbalanced astral microtubules. Importantly, as latrunculin B also delayed the onset of sister chromatid separation, we termed this phenomenon a spindle orientation checkpoint (SOC) (Gachet *et al*, 2001). We speculated that actin depolymerisation might activate a mitotic checkpoint by disrupting the reorganisation of the actin cytoskeleton that accompanies entry into mitosis. As cells enter mitosis, actin disappears from the tips of the cells and relocates around the early mitotic nucleus to form the cytokinetic actomyosin ring (CAR), whose constriction directs the assembly of the cytokinetic septum (Marks and Hyams, 1985). We postulated that the CAR is necessary for the positioning of proteins or protein complexes that mediate the dynamic interaction of the growing ends of astral microtubules with the medial cell cortex, and that disruption of this structure activates the SOC. In the present study, we have addressed this hypothesis directly by simultaneously comparing chromosome separation, astral microtubule behaviour and spindle orientation in living cells in the presence or absence of latrunculin B, and in mutants in which either the actomyosin ring is disorganised or the dynamic association of astral microtubules with the spindle pole body is disturbed. In doing so, we have uncovered a role for Mid1 in directing perpendicular alignment of the mitotic spindle to the axis of cell division and demonstrate that this process is monitored by a checkpoint that regulates the onset of anaphase.

Results

Latrunculin inhibits spindle rotation, spindle elongation and anaphase onset

We have made use of a fission yeast strain in which the non-essential $\alpha 2$ -tubulin gene *atb2* is tagged with GFP (Ding *et al*, 1998). We first determined whether the SOC was functional in *gfp-atb2* cells. Synchronous G2 cells were transferred into fresh medium with or without latrunculin B (Gachet *et al*, 2001). Control cells initiated anaphase at 20 min, reaching a peak at 60 min. In the presence of 10 μ M latrunculin B, the increase in binucleate cells was substantially delayed, reaching a peak only after ~ 2.5 h (Figure 1A). Examination of living cells revealed that the initiation of mitosis (appearance of a mitotic spindle) in latrunculin B was the same as in untreated cells, but that the time spent with a short spindle and unsegregated chromosomes was extended, confirming our previous observations using fixed preparations (Gachet

et al, 2001). To examine spindle orientation and chromosome dynamics simultaneously, we followed individual *gfp-atb2* cells through mitosis in a medium that also contained DAPI. In the sequence of a control cell shown in Figure 1B (upper panel) (Supplementary Movie 1), images were first taken as the spindle forms during phase 1. Time zero is shown as the beginning of phase 2 when the spindle length becomes constant (Figure 1B upper panel and 1D). Phase 2 lasted ~ 9 min, during which the spindle rapidly orients toward the longitudinal axis of the cell (Figure 1C and D). We noted that in control cells anaphase A was only initiated once the spindle angle was less than 30° with respect to the cell axis, and full orientation was accomplished in early phase 3 (Figure 1B and C). Anaphase A and anaphase B commenced co-incidentally, as previously described (Figure 1D). The rate of anaphase B was $0.51 \mu\text{m min}^{-1}$ (Figure 1D), comparable to that recorded by others (Nabeshima *et al*, 1998; Mallavarapu *et al*, 1999; Yamamoto *et al*, 1999). In the presence of latrunculin B, the mitotic spindle remained at an oblique angle to the cell axis for more than 20 min (Figure 1B lower panel and 1C) (Supplementary Movie 2). Chromosome segregation was delayed until 17.5 min, by which time the spindle had elongated from 2.4 to 3.1 μm (Figure 1B lower panel and 1D). Following chromosome segregation, the rate of spindle elongation was significantly slower at $0.30 \mu\text{m min}^{-1}$ than the control (Figure 1D). The observation that spindle length increases during phase 2 in latrunculin B was confirmed in more than 50 cells examined. Furthermore, no relationship between the timing of chromosome segregation and spindle angle was detected. In these cells, the spindle eventually oriented during phase 3, possibly as a result of interaction of spindle pole bodies with the cell cortex.

Latrunculin disrupts cortical capture of astral microtubules

A further difference noted in movies of *gfp-atb2* cells was the behaviour of the astral microtubules. To facilitate the acquisition of clearer, more frequent images, we filmed cells in the absence of DAPI (control cells 94 frames, latrunculin-treated cells 104 frames). One such sequence is shown in Figure 2A (Supplementary Movie 3). The length of the astral microtubule bundle from each SPB was measured (Figure 2B). Three periods are highlighted. During period I ($t = 60\text{--}130$ s), astral microtubules from both upper and lower SPBs contact the cell cortex and this results in a reduction of spindle angle from approximately 50 to 30° (Figure 2B). During period II ($t = 130\text{--}172$ s), the upper astral microtubule shrinks and loses contact with the cortex and no further orientation of the spindle is seen, even though the lower astral microtubule retains cortical contact (Figure 2B). During period III ($t = 172\text{--}245$ s), the astral microtubule from the upper SPB re-establishes cortical contact and the spindle rapidly orients. Thus, spindle orientation primarily occurs when astral microtubules from both poles simultaneously contact opposite sides of the cell cortex (Figure 2C). These interactions are first visible in phase 2, when spindle length is less than $2.5 \mu\text{m}$, but continue until full orientation of the spindle is accomplished in early phase 3. Similar results were obtained in over 20 mitotic cells. From merged images from Figure 2A, we find that, during early mitosis, the astral microtubules interact with the medial cortical region in a region that we

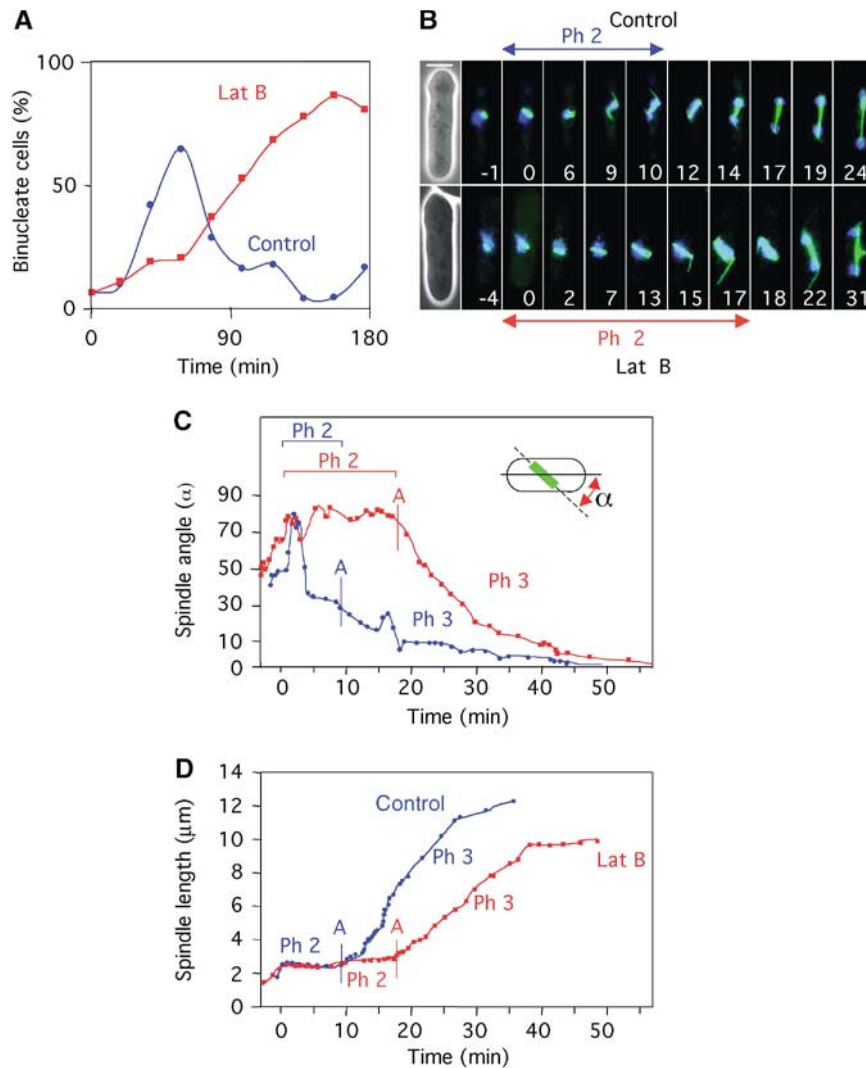


Figure 1 Microtubule dynamics and timing of chromosome separation are affected in the presence of latrunculin B. (A) Synchronous *gfp-atb2* cells were placed in fresh medium containing DAPI either in the absence (blue circles) or presence (red squares) of 10 μ M latrunculin B. The percentage of binucleate cells at various times is shown. (B) Microtubule dynamics in *gfp-atb2* cells in the absence (upper panel) (Supplementary Movie 1) or presence (lower panel) (Supplementary Movie 2) of latrunculin B. Numbers indicate time in minutes from the start of phase 2. Bar = 4 μ m. (C) Analysis of spindle angle relative to the long cell axis and (D) spindle length in control cells (blue circles) and latrunculin B-treated cells (red squares) (from Supplementary Movies 1 and 2). The onset of chromosome segregation (anaphase A) is shown by a vertical blue bar in control cells and a vertical red bar in latrunculin B-treated cells.

call the ‘astral microtubule interaction zone’ (AMIZ) (Figure 2C and D).

In early mitosis, astral microtubules underwent rapid changes in growth and shrinkage and were nucleated at multiple angles to the mitotic spindle (Figure 2A). During spindle elongation, astrals became more stable in length, were thicker (possibly due to microtubule bundling) and remained at a fixed angle (Figure 2A). We repeated this analysis in cells treated with latrunculin B. In these cells, astral microtubules made more erratic transitions between phases of growth and shrinkage. These astrals did not appear to contact the cell cortex and were ineffective in orienting the spindle (Figure 2E and F) (Supplementary Movie 4). These data strongly suggest that astral microtubules impose a ‘rotational force’ in early mitosis that drives the SPBs away from the cell cortex. Whether the slower rate of spindle elongation in latrunculin B indicates that astral microtubules also contribute to a force during anaphase B that helps drive

the SPBs towards the cell tips is at present unknown, although the pioneering experiments of Aist *et al* (1991) suggest that such a possibility should not be discounted.

Astral microtubules control spindle dynamics and anaphase onset

To investigate the involvement of astral microtubules in spindle positioning, we analysed the mutant *cdc11-123* in which association of astral microtubules with the SPBs is defective (Krapp *et al*, 2001). We found that, in *cdc11-123 gfp-atb2* at a semipermissive temperature, 96% of metaphase and 26% of anaphase spindles were misoriented (Table I). In addition, phase 2 was extended in *cdc11-123 gfp-atb2* cells (14 ± 2 min) relative to that observed in wild-type cells (9 ± 1 min) at the same temperature (Figure 3A and Table I). Furthermore, in *cdc11-123 gfp-atb2* cells, the spindle underwent numerous small but rapid oscillations in angle during phase 2, but these were ineffective in rotating the spindle

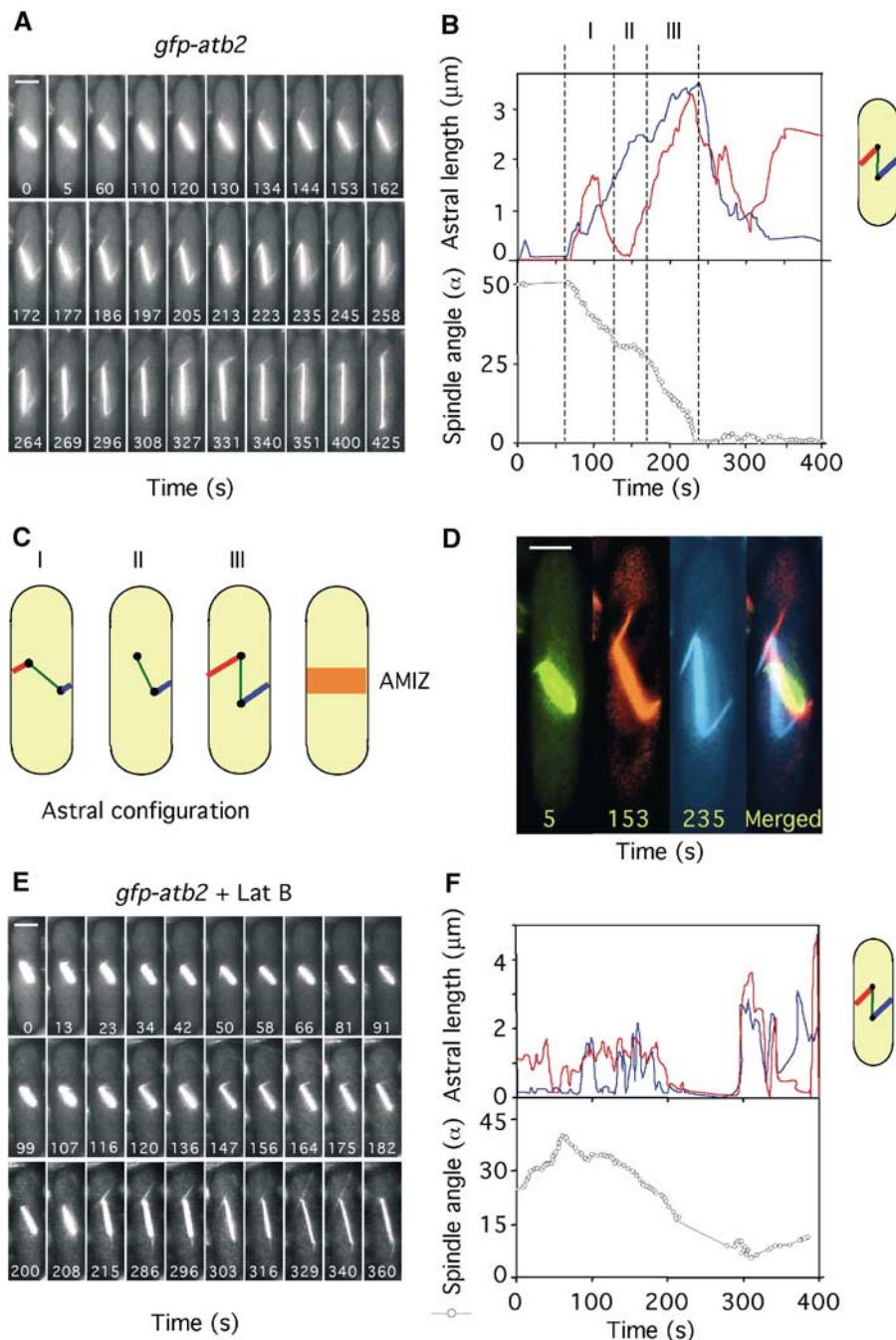


Figure 2 Spindle orientation requires balanced interaction of astral microtubules with the medial cell cortex. **(A)** Microtubule dynamics in *gfp-atb2* cells in medium lacking DAPI (Supplementary Movie 3). Numbers indicate time in seconds from the beginning of the movie. **(B)** Analysis of astral microtubule length (upper panel) and spindle angle (open circles, lower panel) was carried out as depicted in Supplementary Movie 3. Astral microtubule length from the upper SPB (red) or lower SPB (blue) to the cell cortex is shown. Three periods are highlighted: period I ($t = 60\text{--}130$ s), period II ($t = 130\text{--}172$ s) and period III ($t = 172\text{--}245$ s). **(C)** Cartoon showing astral microtubule configurations during periods I–III. The point of interaction of the astral microtubules with the cell cortex defines an AMIZ surrounding the nucleus. **(D)** Frames 5, 153 and 235 from Supplementary Movie 3 were enlarged to illustrate the point of interaction of the astral microtubules from the upper and lower SPBs with the medial cell cortex (Bar = 2 μm). **(E)** Microtubule dynamics in *gfp-atb2* cells in the presence of 10 μM latrunculin B (Supplementary Movie 4). **(F)** Astral microtubule length (upper panel) and spindle angle (lower panel) were determined from Supplementary Movie 4 as detailed above.

(Figure 3A and B) (Supplementary Movie 5). Indeed, astral microtubules were difficult to visualise in *cdc11-123* cells, making short, nonproductive excursions from the SPBs (Figure 3A), and those associated with longer spindles were also abnormal (Frame 19.6, Figure 3A). These data suggest that *cdc11-123* cells show an inherent activation of the SOC and that astral microtubules are required both

for spindle orientation and for determining the timing of sister chromatid separation in fission yeast. The eventual rate of spindle elongation during phase 3 in these cells was $0.37 \pm 0.01 \mu\text{m min}^{-1}$ (Table I), slower than control cells and again raising the possibility that astral microtubules also contribute to the rate of spindle elongation (see above).

Table I Spindle orientation, elongation and timing of anaphase onset

	Frequency of misoriented spindles (%)		Length of phase 2 (min)	Rate of spindle elongation ($\mu\text{m min}^{-1}$)
	Before anaphase	After anaphase		
<i>wt</i>	30	5	9 \pm 1	0.51 \pm 0.04
<i>wt</i> + Lat B	52	27	18 \pm 4	0.30 \pm 0.02
<i>cps8-188</i>	92	28	24 \pm 4	0.31 \pm 0.02
<i>myo52</i> Δ	75	30	52 \pm 23 ^a	0.26 \pm 0.05
<i>myo51</i> Δ	87	40	24 \pm 2	0.28 \pm 0.03
<i>cdc11-123</i>	96	26	14 \pm 2	0.37 \pm 0.01

Percentage of misoriented spindles before and after chromosome separation in control cells (*wt*) or cells treated with latrunculin B (*wt* + Lat B) and in *cps8-188*, *myo51* Δ , *myo52* Δ , *cdc11-123* and *mid1* Δ mutants. $n = 200$ in each case. Statistical analysis of the timing of anaphase onset and rate of spindle elongation in wild type ($n = 20$), wild type + Lat B ($n = 9$), *cps8-188* ($n = 6$), *myo51* Δ ($n = 7$), *myo52* Δ ($n = 8$) and *cdc11-123* ($n = 9$). The error denotes standard error from the mean (SEM).

^aExaggerated anaphase delay is partially due to altered cell polarity.

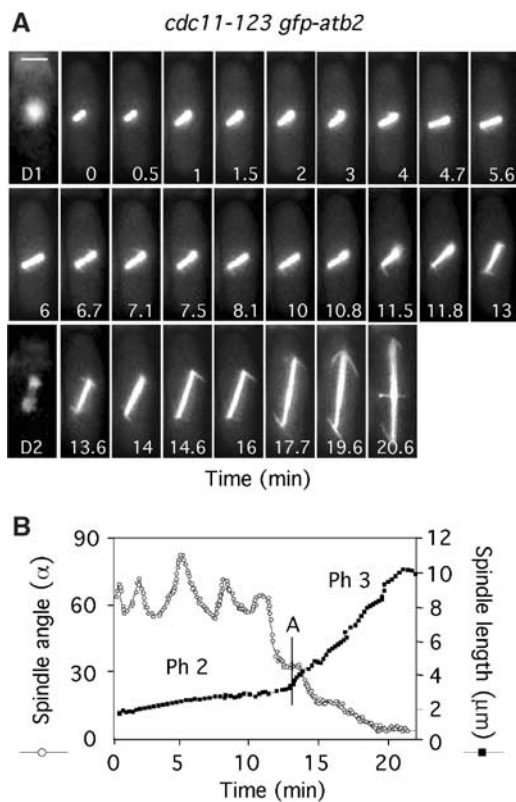


Figure 3 Astral microtubules regulate spindle orientation, spindle elongation and the timing of anaphase onset. (A) *cdc11-123 gfp-atb2* cells were filmed in medium containing Hoechst (Supplementary Movie 5). Numbers indicate the time from when the spindle attained 2 μm . Bar = 4 μm . D1 ($t = 0$) and D2 ($t = 13.6$) are images of chromatin staining. (B) Analysis of the changes in spindle angle (open circles) and spindle length (closed squares) (Supplementary Movie 5). The vertical bar denotes the time of chromosome separation (anaphase A).

The medial actin cytoskeleton regulates spindle positioning

We previously argued that the effect of latrunculin B on mitosis results from the displacement of an actin-containing protein complex at the medial cell cortex, which is necessary for productive astral microtubule interactions (Gachet *et al*, 2001). To examine this possibility, we initially observed microtubule dynamics in the actin mutant *cps8-188* (Ishiguro and Kobayashi, 1996). Analysis of *cps8-188 gfp-*

atb2 cells showed that phase 2 was considerably longer (24 \pm 4 min; $n = 9$) than in wild-type cells at the same temperature (Figure 4A and B, Table I). During this time, the spindle extended from ~ 2.0 to 3.5 μm in the absence of chromosome separation (Figure 4A and B). Anaphase B was initiated as chromosomes separated, and was similar in rate to that observed in wild-type cells treated with latrunculin B (Table I). Importantly, astral microtubules and spindle oscillations were virtually absent in these cells both before and after sister chromatid separation (Figure 4A and B) (Supplementary Movie 6). Statistical analysis showed that in wild-type cells, only 30% of spindles were misoriented prior to chromosome separation (i.e. greater than 30 $^\circ$ to the cell axis) and less than 5% remained misoriented during anaphase B (Table I). By contrast, the proportion of misoriented spindles was greatly increased either in cells treated with latrunculin B or in the *cps8-188* mutant (Table I). These data suggest that the effect of latrunculin B on mitosis in fission yeast is through its well-documented role as an actin-depolymerising agent (Ayscough *et al*, 1997).

In fission yeast, actin relocates from the cell tips to the medial cell cortex in early mitosis as the spindle forms. To examine whether this is required for spindle positioning, we arrested a cold-sensitive α -tubulin mutant *nda2-KM52* by growth at 20 $^\circ\text{C}$ (Toda *et al*, 1984). These cells arrest in a pre-metaphase state with the type II myosin Myo2 (Mulvihill *et al*, 2001) at the medial cell cortex (Figure 4C). When cells were returned to the permissive temperature in the presence of latrunculin B, they showed a significant delay in chromosome separation (Figure 4D). We also observed spindle-positioning defects and a delay in anaphase onset in cells lacking the formin For3, which have actin patches but lack actin cables (Feierbach and Chang, 2001; data not shown). These data suggest that the medial actin cytoskeleton and, in particular, actin cables are required both for spindle rotation and the timing of anaphase onset.

Two type V myosins are required for spindle positioning and anaphase onset

We next examined microtubule dynamics and the timing of sister chromatid separation in mutants of CAR components. We focused initially on the strain *myo52* Δ (delete brackets) lacking the fission yeast type V myosin Myo52, which relocates from the cell poles to the CAR in the M phase (Motegi *et al*, 2001; Win *et al*, 2001). Initial analysis revealed that 75% of metaphase and 30% of anaphase spindles were

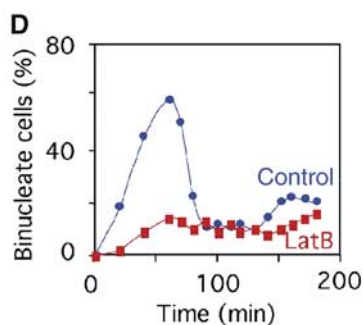
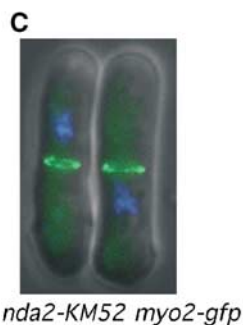
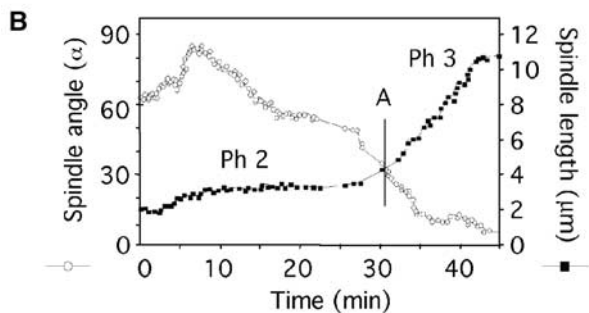
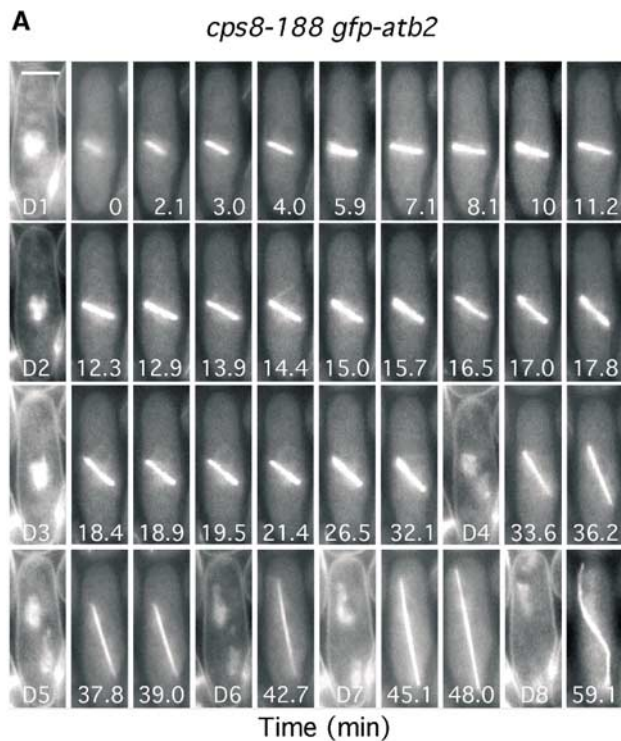


Figure 4 The medial cortical actin cytoskeleton regulates spindle orientation, spindle elongation and the timing of anaphase onset. (A) *cps8-188 gfp-atb2* cells were filmed in medium containing Hoechst (Supplementary Movie 6). Numbers indicate the time from when the spindle attained 2 μm . Bar = 4 μm . D1–D8 are images of chromatin staining. (B) Analysis of the changes in spindle angle (open circles) and spindle length (closed squares) in *cps8-188 gfp-atb2* cells (Supplementary Movie 6). The vertical bar denotes the time of chromosome separation (anaphase A). (C) *nda2-KM52 myo2-gfp* cells arrested at 20°C for 6 h. Cells were visualised for GFP (green) and chromatin (blue). (D) *nda2-KM52* cells were arrested at 20°C for 6 h and released at the permissive temperature (29°C) in the presence (red squares) or absence (blue circles) of 10 μM latrunculin B. The percentage of binucleate cells at various times was determined.

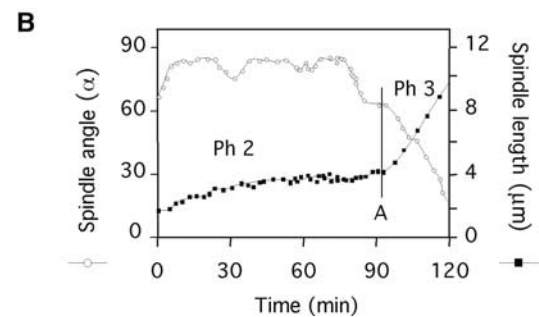
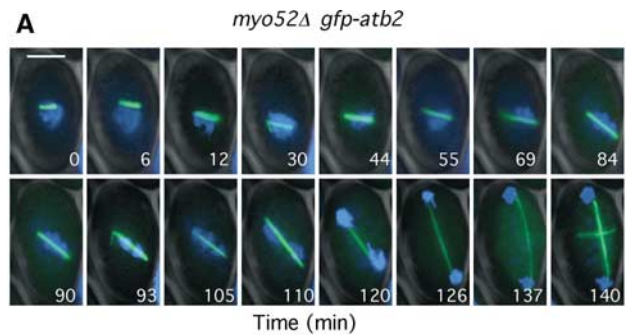


Figure 5 The spindle orientation checkpoint is activated by disruption of the CAR. (A) *myo52 Δ gfp-atb2* cells were filmed in medium containing Hoechst (Supplementary Movie 7). Numbers indicate the time from when the spindle attained 2 μm . Bar = 4 μm . (B) Analysis of spindle angle (open circles) and spindle length (closed squares) in *myo52 Δ gfp-atb2* cells (Supplementary Movie 7). The vertical bar denotes the time of chromosome separation (anaphase A).

misoriented in *myo52 Δ gfp-atb2* cells (Table I), and that these cells showed a variable but extended (52 ± 23 min) delay over anaphase onset (Figure 5A and B, Table I). This suggests that cells lacking Myo52 exhibit an intrinsic activation of the SOC. In the sequence shown in Figure 5B, the spindle remained oriented at $\sim 90^\circ$ to the cell axis and doubled in length in the absence of sister chromatid separation (Figure 5A and B) (Supplementary Movie 7). Notably, astral microtubules were absent in these cells both before and after chromosome segregation. The rate of spindle elongation was $0.26 \pm 0.05 \mu\text{m min}^{-1}$, similar to that seen in latrunculin B-treated cells (Table I). Together, these data suggest that the SOC is activated in *myo52 Δ* cells. Myo52 is involved not only in septum formation but also in the maintenance of growth polarity. We repeated this analysis in *myo51 Δ* cells that lack the second fission yeast type V myosin Myo51, which is also a component of the CAR but has no role in controlling interphase cell polarity (Win *et al*, 2001). *myo51 Δ gfp-atb2* cells displayed a high level of misoriented spindles, 87% before and 40% after anaphase onset, as well as an extended (24 ± 2 min) delay over anaphase onset (Table I). We conclude that, as in budding yeast (Beach *et al*, 2000; Yin *et al*, 2000), type V myosins play an important role in spindle rotation.

Astral microtubules from only one SPB contact the CAR

To examine more accurately where astral microtubules interact with the cell cortex, we monitored microtubule dynamics in *cdc15-gfp gfp-atb2* cells. Cdc15 is required for the reorganisation of F-actin at mitosis and locates solely to the CAR in mitotic cells (Fankhauser *et al*, 1995). At the beginning of the movie, a short mitotic spindle has formed and Cdc15 is

located in a discrete ring structure at the cell periphery, where it remains throughout the filming period (Figure 6A) (Supplementary Movie 8). At $T = 54$ s, an astral microtubule emanating from the lower SPB interacts with the medial cell cortex distal to the CAR. At $T = 66$ s, the astral microtubule is swept towards the Cdc15 ring and then contracts after making brief contact (Figure 6A) (Supplementary Movie 8). After 4 s, chromosomes separate ($T = 70$ s). At $T = 168$ s, an astral microtubule from the same SPB contacts the medial cell cortex and then again associates with the Cdc15 ring at $T = 172$ s (Figure 6A) (Supplementary Movie 8). The position of the spindle was mapped relative to the position of the CAR by kymographic analysis during spindle elongation (Figure 6B) (Supplementary Movie 8). Whereas the CAR remained fixed in the central plane of the cell, the spindle moved relative to it, particularly after the interaction of astral microtubules with the CAR (Figure 6B). Throughout the movie, spindle poles remained on opposite sides of the CAR. We have observed that in 19 out of 19 movies of *cdc15-gfp gfp-atb2* cells, an astral microtubule from only one SPB associates with the Cdc15 ring (data not shown). As we have imaged only one plane through the z-axis of the cell, we cannot rule out the possibility that an astral microtubule from the other SPB also associates with the CAR,

although this was never observed. Additionally, in 15 out of 19 of these movies, we found that anaphase occurs less than 10 s after an astral microtubule first contacts the CAR. In the remaining four movies, an astral microtubule contacts the CAR only after anaphase (data not shown). In these cells, an astral microtubule may contact the CAR prior to anaphase onset but out of the plane of image acquisition. Finally, we noted that in all movies astral microtubules polymerise from the SPB to only one side of the cell cortex in early mitosis, and are nucleated in both directions (i.e. an antiparallel manner) to contact both sides of the cell cortex as spindles elongate. We presume that this enables astral microtubules to stabilise spindle alignment along the longitudinal axis of the cell.

The anillin homologue *Mid1* stabilises alignment of the mitotic spindle

The anillin homologue *Mid1* is required to place the division septum perpendicularly to, and in the centre of, the dividing fission yeast cell. In the absence of *Mid1*, the CAR is placed both at random angles and random positions in the cell (Chang *et al*, 1996; Sohrmann *et al*, 1996). This prompted us to investigate whether the position of the CAR is important for spindle rotation or the timing of anaphase onset. Analysis

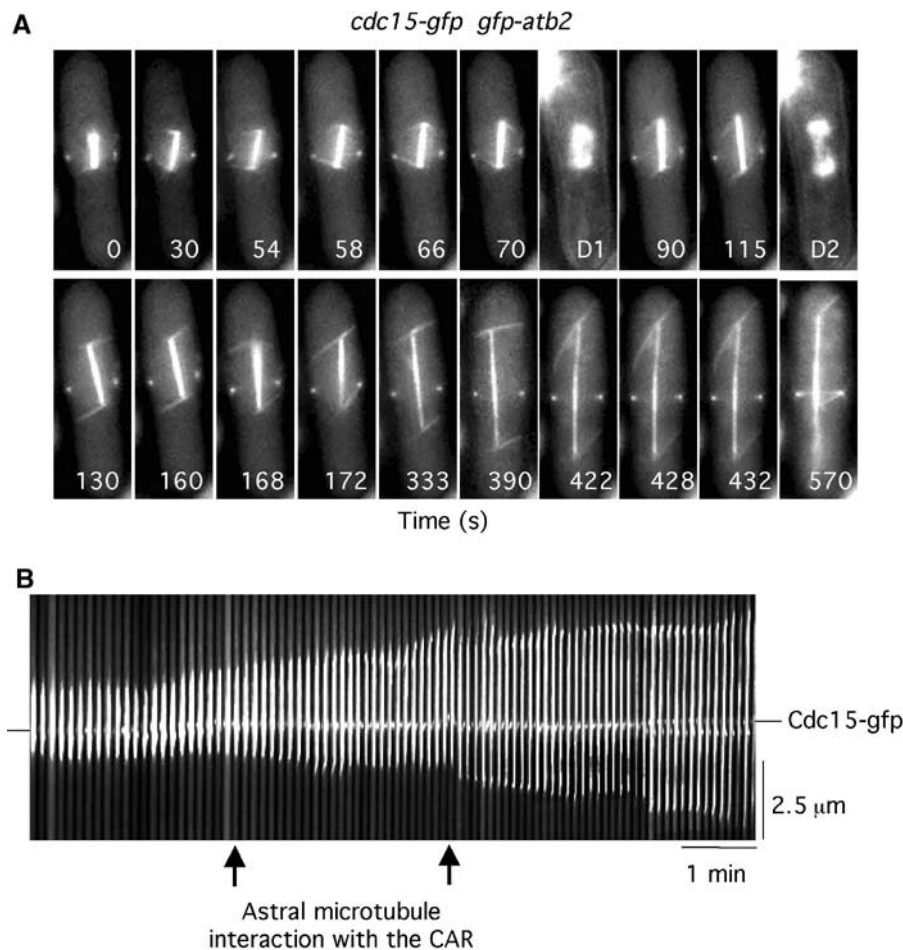


Figure 6 Astral microtubules interact with the CAR. (A) *cdc15-gfp gfp-atb2* cells were filmed in medium containing Hoechst. Numbers indicate the time from the beginning of the movie (Supplementary Movie 8). D1 and D2 are images of chromatin staining. (B) Kymographic analysis of spindle position relative to the CAR in *cdc15-gfp gfp-atb2* cells. In all, 100 images are shown (each 4 pixels wide). Arrows indicate the point of interaction of the astral microtubule from the lower SPB with the cortex.

of spindle rotation in *mid1Δ gfp-atb2* cells revealed that spindles rotated to within 30° of the longitudinal axis of the cell, but failed to stabilise at 0° (i.e. perpendicularly to the division axis), as is observed in wild-type cells (Figure 7A and B). Indeed, multiple rapid oscillations were observed during the filming period (Figure 7A and B). Association of astral microtubules with the cell cortex and spindle rotation in *mid1Δ* cells was blocked by the addition of latrunculin B (data not shown). These results suggest that interaction of astral microtubules with the AMIZ directs gross spindle rotation, and interaction of one astral microtubule with the CAR ensures that spindles are aligned perpendicular to the division axis. Importantly, we also find that in *mid1Δ* cells, phase 2 is longer (26 min) and the rate of spindle elongation slower ($0.36 \mu\text{m min}^{-1}$) than in wild-type cells (Figure 7A and B). This suggests that interaction of astral microtubules with the CAR determines the timing of anaphase onset.

Mid1 is housed in the interphase nucleus and relocates to a broad medial cortical region, which overlaps with the AMIZ) in early M phase and co-localises with the division septum during cytokinesis (Bahler *et al*, 1998; Paoletti and Chang, 2000; Figure 7C). To determine whether the cortical actin cytoskeleton is required for relocalisation of Mid1, synchronised *mid1-gfp* cells were treated with latrunculin B. We find that Mid1 relocates to the AMIZ in the presence of latrunculin, although contraction into the CAR does not occur (Figure 7A). These data suggest that localisation of actin and Mid1 to the AMIZ is mutually independent. However, localisation of Mid1 to the CAR is dependent on actin and, conversely, actin does not concentrate at the centre of the AMIZ in the absence of Mid1. We conclude that the co-ordination of spindle position with the axis of cell division is initiated at the G2/M transition and that Mid1 is an early cortical landmark in this process.

Discussion

In fission yeast, as in animal cells, the mitotic spindle is positioned perpendicular to the axis of cell division during mitosis. We have investigated as to how this is achieved by live analysis of *gfp-atb2* cells. In control cells, astral microtubules emanate from both SPBs in multiple directions and oscillate rapidly between growth and shrinkage. Astral microtubule ends initially associate with the cell cortex in a 3 μm wide medial band surrounding the nucleus. We have termed this an AMIZ (Figures 2 and 8). Contacts with the AMIZ are initiated as the spindle forms and continue during phase 2 of mitosis. Spindle rotation appears to occur only when astral microtubules from both SPBs simultaneously and oppositely contact the cell cortex. Several lines of evidence indicate that these interactions are a prerequisite for spindle rotation. First, we show that spindle rotation is delayed in *cdc11-123* mutants in which proper nucleation of astral microtubules at the SPB is disturbed (Krapp *et al*, 2001). Second, we show that spindle orientation is prevented by disruption of the medial actin cytoskeleton, either by addition of latrunculin B or the actin mutant *cps8-188*. Third, we show that two type V myosins, Myo51 and Myo52, that locate to the medial cell cortex in the M phase are necessary for spindle rotation. Strikingly, under every condition in which we observed defective spindle orientation, astral microtubule dynamics were also perturbed. Hence, the AMIZ may act as a regulator of astral

microtubule dynamics at the cell equator in the same way that complexes at cell tips that contain the kelch-domain containing protein Tea1 regulate the dynamic properties of cytoplasmic microtubules during interphase (Mata and Nurse, 1997). We conclude that astral microtubules interact with actin cables at the medial cell cortex via type V myosins to direct gross spindle rotation in fission yeast.

In addition, we noted that, by live analysis of *cdc15-gfp gfp-atb2* cells, astral microtubules from one of the two poles were captured at the AMIZ and then moved towards the CAR, which is situated at the centre of the AMIZ. To examine whether the position of the CAR is important for spindle positioning, we examined spindle position in the absence of Mid1, which is required for placement of the division septum in the centre of the cell, and perpendicular to its longitudinal axis. We find that, in the absence of Mid1, spindles rotate but fail to stabilise along the longitudinal axis of the cell. The rapid oscillations of the spindle in *mid1Δ* cells are probably due to continued interaction of astral microtubules with the AMIZ, as addition of latrunculin abolishes further spindle rotation. We presume that interaction of astral microtubules with the CAR also maintains the SPBs on opposite sides of the CAR, as this geometry is abolished in the absence of Mid1. Thus, we can define two separate elements that are required for spindle positioning: an early component that causes gross spindle rotation and requires simultaneous contact of astral microtubules with the AMIZ, and a later component that stabilises correct alignment of the spindle and that requires interaction of an astral microtubule from at least one of the two SPBs with the CAR.

Prior to cell division in budding yeast, the mitotic spindle is re-positioned across the bud neck by the action of cytoplasmic microtubules that emanate from the outer plaque of the duplicated SPBs. At least two pathways mediate capture of the cytoplasmic microtubule 'plus' ends by both the bud neck and the cell cortex underlying the bud tip (Bloom, 2000). Early in the cell cycle, Kar9 mediates the capture of cytoplasmic microtubules by actin cables through its association to type V myosin, serving to orient the mitotic spindle towards the bud neck (Adames and Cooper, 2000; Yeh *et al*, 2000; Kusch *et al*, 2002). Kar9 resides on the 'plus' end of cytoplasmic microtubules via its association to the microtubule-binding protein Bim1, an EB1 homologue (Miller *et al*, 2000). During anaphase, dynein mediates lateral interactions between microtubules and the cell cortex to pull the nucleus into the bud (Muhua *et al*, 1994; Cottingham and Hoyt, 1997; Adames and Cooper, 2000). In agreement with this, spindle positioning is sensitive to actin-depolymerising agents early but not late in the cell cycle (Theesfeld *et al*, 1999). In some respects, our data appear to mirror events in budding yeast, where microtubule capture by the cleavage apparatus is required for proper spindle positioning (Kusch *et al*, 2002). Indeed, some elements of the spindle orientation mechanism are undoubtedly conserved between budding and fission yeasts, such as actin, Myo52/Myo2 and Cdc11/Nud1 (Gruneberg *et al*, 2000; Yin *et al*, 2000). However, fission yeast contains no obvious Kar9 orthologue, and other molecules, such as cytoplasmic dynein, which is central to the nuclear positioning mechanism in budding yeast (Carminati and Stearns, 1997; Heil-Chapdelaine *et al*, 2000) and mammalian cells (O'Connell and Wang, 2000), are thought to play no such role in fission yeast. This may be either because the

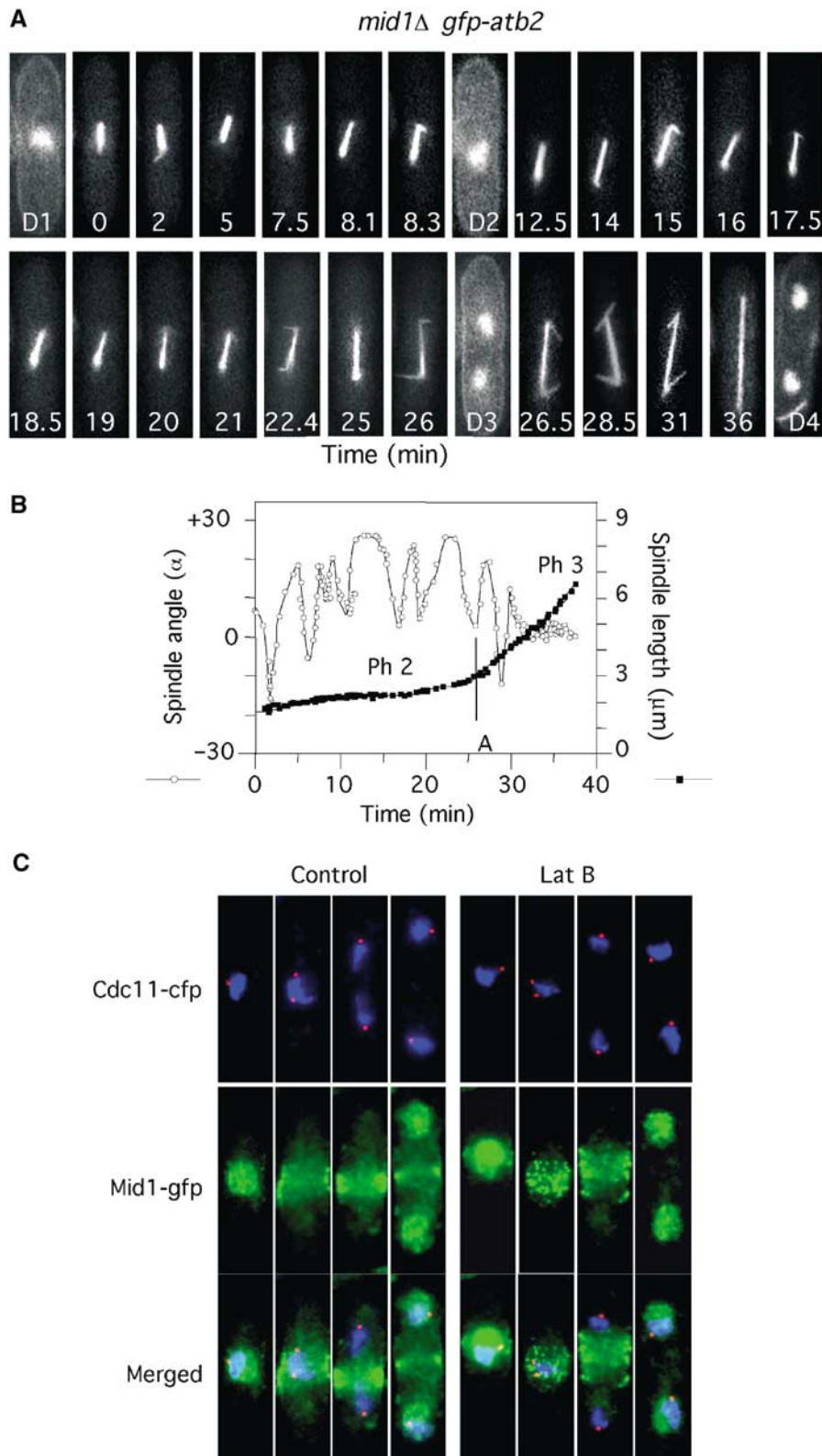


Figure 7 Mid1 stabilises spindle alignment to the longitudinal axis of the cell. (A) *mid1Δ gfp-atb2* cells were filmed in medium containing Hoechst. Numbers indicate the time from when the spindle attained 2 μm . D1–D4 are images of chromatin staining. (B) Analysis of the changes in spindle angle (open circles) and spindle length (closed squares) from (A). The vertical bar denotes the time of chromosome separation (anaphase A). (C) Synchronous *mid1-gfp cdc11-cfp* cells placed in fresh medium containing Hoechst either in the absence (left panels) or presence (right panels) of 10 μm latrunculin B. Images were taken to visualise Cdc11-CFP (red), Mid1-GFP (green) or chromatin (blue) when cells were in G2 (single SPB), metaphase (separated SPBs but unseparated chromatin), anaphase (separated SPBs and separated chromatin) and telophase.

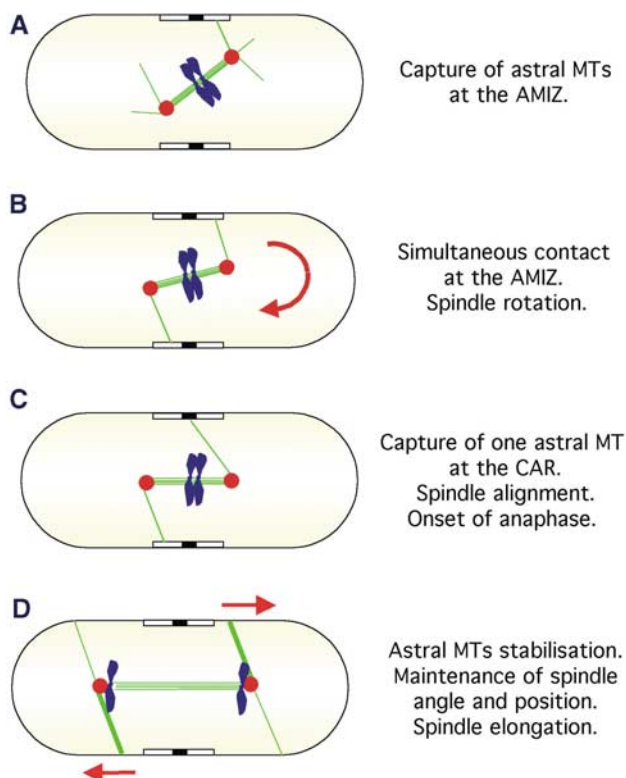


Figure 8 Model illustrating the function of astral microtubules in fission yeast. **(A)** In wild-type cells, the spindle forms at a random angle to the cell axis. **(B)** Astral microtubules (green lines) that polymerise from the extranuclear face of the SPBs (red circles) interact with a zone that surrounds the nucleus, which we term an AMIZ (open box). Spindle rotation is driven by simultaneous contact on both sides of the cell cortex. **(C)** An astral microtubule from one SPB contacts the CAR (closed box). This stabilises alignment of the spindle along the longitudinal axis of the cell. **(D)** Spindle elongation (anaphase B) and separation of sister chromatids (blue) occur co-incidentally. Astral microtubules maintain spindle angle and contribute to the rate of spindle elongation during anaphase B.

fission yeast nucleus is positioned correctly prior to mitosis or that dynein function is restricted to the fission yeast meiotic cell cycle (Yamamoto *et al*, 1999; Miki *et al*, 2002).

In fission yeast, spindles remain at a constant length during phase 2 of mitosis and anaphase A occurs concurrently with the onset of anaphase B. This normally occurs only when the spindle achieves an angle of approximately 30° or less to the longitudinal axis of the cell. Several lines of evidence suggest that failure to achieve this angle leads to activation of a spindle orientation checkpoint that delays the onset of anaphase (Gachet *et al*, 2001). Firstly, disruption of astral microtubule interaction with the medial cell cortex leads to spindle elongation during phase 2 and a delay in the separation of sister chromatids. Spindle elongation observed during phase 2 in this situation is likely to be due to pushing forces provided by interdigitated pole-to-pole microtubules, but this is slow and may reflect counter forces resulting from persistent attachment of microtubules to un-separated sister chromatids. Secondly, when astral microtubule contact with the cell cortex is disturbed, the relationship between spindle orientation and sister chromatid separation seen in wild-type cells breaks down in that anaphase occurs when the spindle is at angles of up to 70° relative to the

longitudinal axis of the cell. Such aberrant mitoses are always preceded by a delay in sister chromatid separation, namely an extension of Phase 2. This confirms our previous conclusion that in fission yeast, spindle position is monitored by a checkpoint that regulates the onset of anaphase (Gachet *et al*, 2001). This contrasts directly with the situation in budding yeast, in which spindle mis-positioning activates a checkpoint that delays the onset of cytokinesis (Bardin *et al*, 2000, Adames *et al*, 2001, Lee *et al*, 2001). The reason for this difference is at present unknown.

In higher eukaryotic cells, many models have been proposed to explain the relative position of the spindle and cleavage furrow, but no mechanism has emerged that can generally account for this geometry (Rappaport, 1996; Oegema *et al*, 2000; Glotzer, 2001). Although it is agreed that microtubules are critical for this process, the initial cortical landmarks that dictate the position of the cleavage furrow are unknown. We show that, in fission yeast, the anillin homologue Mid1 is involved in ensuring that the spindle is stably aligned at right angles to the division axis and in the centre of the cell. Mid1 relocates from the nucleus at the G2/M transition to a region on the medial cell cortex that closely corresponds to the AMIZ and is then focused, in an actin-dependent manner, to a ring that co-localises with the CAR (Bahler *et al*, 1998; Paoletti and Chang, 2000). Similarly, in fruit fly and human cells, anillin proteins reside in the nucleus in interphase and relocate to the cell cortex at the G2/M transition, which is focused to a broad ring at metaphase and the cleavage furrow during telophase (Field and Alberts, 1995; Oegema *et al*, 2000). Moreover, inactivation of one of three anillin proteins, by RNAi-mediated gene ablation, leads to spindle-positioning defects in *Caenorhabditis elegans* (Gonczy *et al*, 2000). The cell cycle-dependent relocalisation of Mid1 may partly explain why spindle positioning in fission yeast is determined only in the M phase. Mid1 is homologous to budding yeast BUD4, which is required for bud site selection in haploids and diploids (Chant and Herskowitz, 1991; Sanders and Herskowitz, 1996). Our data raise the possibility that members of the anillin protein family play an evolutionarily conserved role in co-ordinating spindle position with the axis of cell division in all eukaryotes.

Materials and methods

Cell culture

Media, growth, maintenance of strains and genetic methods were as described (Moreno *et al*, 1991). Cultures of *nmt1-gfp-atb2* cells were grown at 25°C in minimal medium, and thiamine was added at a concentration of 3.75 g l⁻¹ in order to repress partially the expression of *gfp-atb2*. Under these conditions, *gfp-atb2* cells grew at a rate indistinguishable from wild type. The strains used in this study are listed in Table II.

Cell synchronisation

Cell synchrony was achieved by lactose gradient size selection. Log-phase cells (50 ml of 2 × 10⁶ cells ml⁻¹) were concentrated in 2 ml and loaded onto a 50 ml 7–35% linear lactose gradient. After 10 min centrifugation at 1600 rpm, 3 ml of the upper of two visible layers was collected and washed twice before being resuspended in fresh medium (0.5 × 10⁶ cells ml⁻¹) at 25°C. At this stage, a 1 ml sample was collected and stained with DAPI to establish the mitotic index. The mean cell size was 11 ± 1 μm, and no spindle was observed (Gachet *et al*, 2001).

Table II Strains used in this study

Strain no.	Genotype	Reference/source
YG 309	<i>h⁻ GFP-nmt1-atb2(lys1)</i>	D-Q Ding
YG 262	<i>h⁺ mid1-GFP::ura4</i>	D McCollum
YG 208	<i>h⁻ cdc11-123</i>	V Simanis
YG 265	<i>h⁻ cdc15-GFP::ura4</i>	V Simanis
YG 166	<i>h⁻ myo2-GFP</i>	Lab stock
YG 277	<i>h⁻ myo52::ura4</i>	Lab stock
YG 128	<i>h⁻ cps8-188</i>	T Toda
YG 125	<i>h⁻ nda2-KM52</i>	Lab stock
YG 779	<i>h⁻ GFP-nmt1-atb2(lys1) cps8-188 ura4⁺ leu1⁺</i>	This study
YG 815	<i>h⁻ GFP-nmt1-atb2(lys1) cdc11-123 ura4⁺ leu1⁺ ade6⁻</i>	This study
YG 744	<i>h⁻ GFP-nmt1-atb2(lys1) myo52::ura4 ade6⁻</i>	This study
YG 1870	<i>h⁻ nda2-KM52 myo2-GFP</i>	This study
YG 847	<i>h⁻ GFP-nmt1-atb2(lys1) cdc15-GFP ura4⁺ leu1⁺ ade6⁻</i>	This study
JM 2610	<i>h⁻ mid1-GFP(ura4) cdc11-CFP::KanR</i>	This study
YG 951	<i>h⁻ GFP-nmt1-atb2(lys1) mid1::ura4 ade6⁻</i>	This study

All strains were *leu1-32 ura4-D18* unless otherwise stated. *ade6⁻* is either *ade6-M210* or *ade6-M216*.

Cell imaging

Live cell analysis of *gfp-atb2* cells used an imaging chamber (CoverWell PCI-2.5, Grace Bio-labs) filled with 1 ml of 1% agarose in minimal medium and sealed with a 22 × 22 mm glass coverslip. An aliquot of cell suspension was applied to the imaging chamber and cells were allowed to equilibrate for 1 h at 25°C before beginning the experiments, which were carried out at this temperature. Latrunculin B was purchased from Calbiochem and used at a concentration of 10 μM. To visualise chromosomes, either 0.1 μg ml⁻¹ DAPI or 0.1 μg ml⁻¹ Hoechst (Molecular Probes) was added to cells for 20 min. Time-lapse images were taken at 5–30 s intervals, with exposure times of 0.2–0.5 s (for GFP) or 0.1 s (for DAPI). The only exception was for *myo52Δ* cells where images were taken every 3 min. In all cases, a single-focal plane image was recorded at each time point. Time zero in the movies is taken to be either the point at which the spindle attains 2 μm or becomes stable in length. Images were visualised with a Hamamatsu C4742 CCD camera fitted to a Zeiss Axiophot microscope with a 64 × 1.4 NA objective, and were recorded using OpenLab software (Improvision Ltd., UK), downloaded to Microsoft Excel for analysis and to Adobe Imageready 3 for assembly into montages.

References

Adames NR, Cooper JA (2000) Microtubule interactions with the cell cortex causing nuclear movements in *Saccharomyces cerevisiae*. *J Cell Biol* **149**: 863–874

Adames NR, Oberle JR, Cooper JA (2001) The surveillance mechanism of the spindle position checkpoint in yeast. *J Cell Biol* **153**: 159–168

Aist JR, Bayles CJ, Tao W, Berns MW (1991) Direct experimental evidence for the existence, structural basis and function of astral forces during anaphase B *in vivo*. *J Cell Sci* **100**: 279–288

Ayscough KR, Stryker J, Pokala N, Sanders M, Crews P, Drubin DG (1997) High rates of actin filament turnover in budding yeast and roles for actin in establishment and maintenance of cell polarity revealed using the actin inhibitor latrunculin-A. *J Cell Biol* **137**: 399–416

Bahler J, Steever AB, Wheatley S, Wang Y, Pringle JR, Gould KL, McCollum D (1998) Role of polo kinase and Mid1p in determining the site of cell division in fission yeast. *J Cell Biol* **143**: 1603–1616

Bardin AJ, Visintin R, Amon A (2000) A mechanism for coupling exit from mitosis to partitioning of the nucleus. *Cell* **102**: 21–31

Beach DL, Thibodeaux J, Maddox P, Yeh E, Bloom K (2000) The role of the proteins Kar9 and Myo2 in orienting the mitotic spindle of budding yeast. *Curr Biol* **10**: 1497–1506

Bloom K (2000) It's a kar9ochore to capture microtubules. *Nat Cell Biol* **2**: E96–E98

Analysis of spindle length, orientation and timing of anaphase onset

The length of the mitotic spindle and its angle with respect to the longitudinal axis of the cell were determined using OpenLab software (Improvision Ltd, UK) for each cell. The timing of nuclear separation was determined visually.

Supplementary data

Supplementary data are available at *The EMBO Journal* Online.

Acknowledgements

We thank Fred Chang, Yasushi Hiraoka, Dan McCollum, and Viesturs Simanis for supplying strains, Vasanti Amin for outstanding technical assistance and Lee Johnston for advice and encouragement. JSH and JBAM are supported by grants from the Wellcome Trust, the Association of International Cancer Research, the Leverhulme Trust, University College London and the Medical Research Council.

Carminati JL, Stearns T (1997) Microtubules orient the mitotic spindle in yeast through dynein-dependent interactions with the cell cortex. *J Cell Biol* **138**: 629–641

Chang F, Woollard A, Nurse P (1996) Isolation and characterization of fission yeast mutants defective in the assembly and placement of the contractile actin ring. *J Cell Sci* **109**: 131–142

Chant J, Herskowitz I (1991) Genetic control of bud site selection in yeast by a set of gene products that constitute a morphogenetic pathway. *Cell* **65**: 1203–1212

Cottingham FR, Hoyt MA (1997) Mitotic spindle positioning in *Saccharomyces cerevisiae* is accomplished by antagonistically acting microtubule motor proteins. *J Cell Biol* **138**: 1041–1053

Dechant R, Glotzer M (2003) Centrosome separation and central spindle assembly act in redundant pathways that regulate microtubule density and trigger cleavage furrow formation. *Dev Cell* **4**: 333–334

Ding D-Q, Chikashige Y, Haraguchi Y, Hiraoka Y (1998) Oscillatory nuclear movement in fission yeast meiotic prophase is driven by astral microtubules, as revealed by continuous observation of chromosomes and microtubules in living cells. *J Cell Sci* **111**: 701–712

Ding R, McDonald KL, McIntosh JR (1993) Three-dimensional reconstruction and analysis of mitotic spindles from the yeast, *Schizosaccharomyces pombe*. *J Cell Biol* **120**: 141–151

Ding R, West RR, Morphew M, Oakley BR, McIntosh JR (1997) The spindle pole body of *Schizosaccharomyces pombe* enters and

- leaves the nuclear envelope as the cell cycle proceeds. *Mol Biol Cell* **8**: 1461–1479
- Fankhauser C, Reymond A, Cerutti L, Utzig S, Hofmann K, Simanis V (1995) The *S. pombe* cdc15 gene is a key element in the reorganization of F-actin at mitosis. *Cell* **82**: 435–444
- Feierbach B, Chang F (2001) Roles of the fission yeast formin for3p in cell polarity, actin cable formation and symmetric cell division. *Curr Biol* **11**: 1656–1665
- Field CM, Alberts BM (1995) Anillin, a contractile ring protein that cycles from the nucleus to the cell cortex. *J Cell Biol* **131**: 165–178
- Gachet Y, Tournier S, Millar JBA, Hyams JS (2001) A MAP kinase-dependent actin checkpoint ensures proper spindle orientation in fission yeast. *Nature* **412**: 352–355
- Glotzer M (2001) Animal cell cytokinesis. *Ann Rev Cell Dev Biol* **17**: 351–386
- Gonczy P, Echeverri C, Oegema K, Coulson A, Jones SJ, Copley RR, Duperon J, Oegema J, Brehm M, Cassin E, Hannak E, Kirkham M, Pichler S, Flohrs K, Goessen A, Leidel S, Alleaume AM, Martin C, Ozlu N, Bork P, Hyman AA (2000) Functional genomic analysis of cell division in *C. elegans* using RNAi of genes on chromosome III. *Nature* **408**: 331–336
- Gruneberg U, Campbell K, Simpson C, Grindlay J, Schiebel E (2000) Nud1p links astral microtubule organization and the control of exit from mitosis. *EMBO J* **19**: 6475–6488
- Hagan IM, Hyams JS (1996) Forces acting on the fission yeast anaphase spindle. *Cell Motil Cytoskel* **34**: 69–75
- Hagan IM, Yanagida M (1997) Evidence for cell cycle-specific, spindle pole body-mediated, nuclear positioning in the fission yeast *Schizosaccharomyces pombe*. *J Cell Sci* **110**: 1851–1866
- Heil-Chapdelaine RA, Tran NK, Cooper JA (2000) Dynein-dependent movements of the mitotic spindle in *Saccharomyces cerevisiae* do not require filamentous actin. *Mol Biol Cell* **11**: 863–872
- Ishiguro J, Kobayashi W (1996) An actin point-mutation neighboring the 'hydrophobic plug' causes defects in the maintenance of cell polarity and septum organization in the fission yeast *Schizosaccharomyces pombe*. *FEBS Lett* **392**: 237–241
- Krapp A, Schmidt S, Cano E, Simanis V (2001) *S. pombe* cdc11p, together with sid4p, provides an anchor for septation initiation network proteins on the spindle pole body. *Curr Biol* **11**: 1559–1568
- Kusch J, Meyer A, Snyder MP, Barral Y (2002) Microtubule capture by the cleavage apparatus is required for proper spindle positioning in yeast. *Genes Dev* **16**: 1627–1639
- Lee SE, Jensen S, Frenz LM, Johnson AL, Fesquet D, Johnston LH (2001) The Bub2-dependent mitotic pathway in yeast acts every cell cycle and regulates cytokinesis. *J Cell Sci* **114**: 2345–2354
- Mallavarapu A, Sawin K, Mitchison T (1999) A switch in microtubule dynamics at the onset of anaphase B in the mitotic spindle of *Schizosaccharomyces pombe*. *Curr Biol* **9**: 1423–1426
- Marks J, Hyams JS (1985) Localisation of F-actin through the cell division cycle of *Schizosaccharomyces pombe*. *Eur J Cell Biol* **39**: 27–32
- Mata J, Nurse P (1997) teal and the microtubular cytoskeleton are important for generating global spatial order within the fission yeast cell. *Cell* **89**: 939–949
- Miki F, Okazaki K, Shimanuki M, Yamamoto A, Hiraoka Y, Niwa O (2002) The 14-kDa dynein light chain-family protein Dlc1 is required for regular oscillatory nuclear movement and efficient recombination during meiotic prophase in fission yeast. *Mol Biol Cell* **13**: 930–946
- Miller RK, Cheng S-C, Rose MD (2000) Bim1p/Yeb1p mediates the Kar9p-dependent cortical attachment of cytoplasmic microtubules. *Mol Biol Cell* **11**: 2949–2959
- Moreno S, Klar A, Nurse P (1991) Molecular genetic analysis of fission yeast *Schizosaccharomyces pombe*. *Meth Enzymol* **194**: 795–823
- Motegi F, Arai R, Mabuchi I (2001) Identification of two type V myosins in fission yeast, one of which functions in polarized cell growth and moves rapidly in the cell. *Mol Biol Cell* **12**: 1267–1380
- Muhua L, Karpova TS, Cooper JA (1994) A yeast actin-related protein homologous to that in vertebrate dynactin complex is important for spindle orientation and nuclear migration. *Cell* **78**: 669–679
- Mulvihill DP, Barretto C, Hyams JS (2001) Localization of fission yeast type II myosin, Myo2, to the cytokinetic actin ring is regulated by phosphorylation of a C-terminal coiled-coil domain and requires a functional septation initiation network. *Mol Biol Cell* **12**: 4044–4053
- Nabeshima K, Nakagawa Y, Straight AF, Murray A, Chikashige Y, Yamashita YM, Hiraoka Y, Yanagida M (1998) Dynamics of centromeres during metaphase-anaphase transition in fission yeast: Dis1 is implicated in force balance in metaphase bipolar spindle. *Mol Biol Cell* **9**: 3211–3225
- O'Connell CB, Wang Y (2000) Mammalian spindle orientation and position respond to changes in cell shape in a dynein-dependent fashion. *Mol Biol Cell* **11**: 1765–1774
- Oegema K, Savoian MS, Mitchison TJ, Field CM (2000) Functional analysis of a human homologue of the *Drosophila* actin binding protein anillin suggests a role in cytokinesis. *J Cell Biol* **150**: 539–552
- Paoletti A, Chang F (2000) Analysis of mid1p, a protein required for placement of the cell division site, reveals a link between the nucleus and the cell surface in fission yeast. *Mol Biol Cell* **11**: 2757–2773
- Rappaport R (1996) *Cytokinesis in Animal Cells*, Vol. 30 Cambridge: Cambridge University Press
- Robinow CF, Marak J (1966) A fiber apparatus in the nucleus of the yeast cell. *J Cell Biol* **29**: 129–151
- Sanders SL, Herskowitz I (1996) The BUD4 protein of yeast, required for axial budding, is localized to the mother/BUD neck in a cell cycle-dependent manner. *J Cell Biol* **134**: 413–427
- Segal M, Bloom K (2001) Control of spindle polarity and orientation in *Saccharomyces cerevisiae*. *Trends Cell Biol* **11**: 160–166
- Sohrmann M, Fankhauser C, Brodbeck C, Simanis V (1996) The dmfl/mid1 gene is essential for correct positioning of the division septum in fission yeast. *Genes Dev* **10**: 2707–2719
- Tanaka K, Kanbe T (1986) Mitosis in the fission yeast *Schizosaccharomyces pombe* as revealed by freeze-substitution electron microscopy. *J Cell Sci* **80**: 253–268
- Tatebe H, Goshima G, Takeda K, Nakagawa T, Kinoshita K, Yanagida M (2001) Fission yeast living mitosis visualized by GFP-tagged gene products. *Micron* **32**: 67–74
- Theesfeld CL, Irazoqui JE, Bloom K, Lew DJ (1999) The role of actin in spindle orientation changes during the *Saccharomyces cerevisiae* cell cycle. *J Cell Biol* **146**: 1019–1032
- Toda T, Adachi Y, Hiraoka Y, Yanagida M (1984) Identification of the pleiotropic cell division cycle gene NDA2 as one of two different alpha-tubulin genes in *Schizosaccharomyces pombe*. *Cell* **37**: 233–242
- Win TZ, Gachet Y, Mulvihill DP, May KM, Hyams JS (2001) Two type V myosins with non-overlapping functions in the fission yeast *Schizosaccharomyces pombe*: Myo52 is concerned with growth polarity and cytokinesis, Myo51 is a component of the cytokinetic actin ring. *J Cell Sci* **114**: 69–79
- Yamamoto A, West R, McIntosh JR, Hiraoka Y (1999) A cytoplasmic dynein heavy chain is required for oscillatory nuclear movement of meiotic prophase and efficient meiotic recombination in fission yeast. *J Cell Biol* **145**: 1233–1249
- Yeh E, Yang C, Chin E, Maddox P, Salmon ED, Lew DJ, Bloom K (2000) Dynamic positioning of mitotic spindles in yeast: role of microtubule motors and cortical determinants. *Mol Biol Cell* **11**: 3949–3961
- Yin H, Pruyne D, Huffaker TC, Bretscher A (2000) Myosin V orientates the mitotic spindle in yeast. *Nature* **406**: 1013–1015